

Field-Theoretic Reggeization in Five- and Six-Point Functions*

B. Balakrishnan

*Laboratory for Nuclear Science and Department of Physics, Massachusetts Institute of Technology, Cambridge, Massachusetts 02139**and Department of Physics, State University of New York at Stony Brook, Stony Brook, New York 11790*

(Received 29 March 1971)

Multiparticle S -matrix elements of the type $N\gamma \rightarrow N\gamma\gamma$, $N\gamma\gamma \rightarrow N\gamma\gamma$ are calculated in the tree approximation, in a field theory of spin- $\frac{1}{2}$ "nucleons" (N) and spin-1 massive "photons" (γ) coupled to the conserved nucleon current. After projecting out the positive-parity amplitude, the asymptotic behavior is found to be consistent with a Reggeized nucleon. The double-Regge-pole limit of $N\gamma \rightarrow N\gamma\gamma$ also indicates a Reggeized nucleon, and the residues factor. The method can be extended to S -matrix elements with arbitrary numbers of photons.

I. INTRODUCTION

The possibility of elementary particles of conventional field theory lying on Regge trajectories was first investigated by Gell-Mann *et al.*¹ for various classes of field theories. In particular, the theory of spin- $\frac{1}{2}$ "nucleons" (N) coupled to spin-1 massive "photons" (γ) through a conserved current was found to yield a Regge trajectory on which the nucleon lies. This was shown by calculating the $\gamma N \rightarrow \gamma N$ amplitude of definite (positive) parity up to sixth order and finding Regge asymptotic behavior.

However, consistent Reggeization requires that the Regge pole be present in all S -matrix elements which contain channels with the quantum numbers of the nucleon, for example, the multiparticle channels $N\gamma$, $N\gamma\gamma$, $N\gamma\gamma\gamma$, etc. The multiparticle amplitudes have not previously been studied in connection with Reggeization, and in this paper we examine the five- and six-point amplitudes $N\gamma \rightarrow N\gamma\gamma$ and $N\gamma\gamma \rightarrow N\gamma\gamma$ in the tree-diagram approximation, testing for Regge asymptotic behavior with fully factored residues.

External spin causes two immediate complications. First, the kinematic singularities of multiparticle amplitudes are not understood. Second, due to the MacDowell symmetry, there are two opposite-parity Regge poles

$$\alpha^\pm(W) = \frac{1}{2} + g^2 f(\pm W) \dots$$

which are degenerate at the tree-approximation level. To handle these complications, we work directly with invariant Feynman amplitudes, making no effort to extract kinematic singularities. The Feynman amplitudes should exhibit Regge-pole factorization in the asymptotic limit. Because of parity doubling it is necessary to isolate positive-parity amplitudes, before an asymptotic limit with a factored Regge nucleon can be expected.

This forces us to work in the timelike region of the total four-momentum carried by the Regge pole, where parity is a "good" quantum number, and where the "natural" partial-wave development is in terms of $O(3)$ harmonics. Our method is to parametrize the amplitudes with $O(3)$ group variables,² project out positive parity in the center-of-mass frame, and take the unphysical asymptotic limit of large cosine to test for Regge behavior. Were it not for parity doubling, an approach based on the $O(2, 1)$ group for spacelike Reggeon momentum, would probably be simpler; but it is awkward to project out definite parity in the $O(2, 1)$ development, because parity does not leave a spacelike vector invariant.

The program is therefore as follows: (a) Look for Regge poles in the $N\gamma \rightarrow N\gamma$ case, and identify the factored residues which describe the coupling $N\gamma \rightarrow$ Reggeon. (b) Look for the same Regge pole in the $N\gamma \rightarrow N\gamma\gamma$ case, and see if the residues factor. One of these factors should be the same as found in (a), while the other should describe the coupling $N\gamma\gamma \rightarrow$ Reggeon. (c) Similarly investigate the $N\gamma\gamma \rightarrow N\gamma\gamma$ case. Both factors describe $N\gamma\gamma \rightarrow$ Reggeon coupling, and should be the same as found in (b). (d) Study the double Regge limit of $N\gamma \rightarrow N\gamma\gamma$, which should contain the same Regge pole twice, and in which two of the factored residues should correspond to $N\gamma \rightarrow$ Reggeon coupling. The third factor corresponds to Reggeon-Reggeon- γ coupling. If this program can be followed through consistently, then we have established the Reggeization of the nucleon for a subset of multiparticle S -matrix elements in lowest order.

II. REVIEW OF THE CASE $N\gamma \rightarrow N\gamma$

We consider the scattering of "nucleons" (spin $\frac{1}{2}$, mass m) and "photons" (spin 1, mass 0) coupled through a conserved nucleon current.

The particles are divided into "in" and "out" clusters (Fig. 1) and the amplitude calculated in their center-of-mass frame.² Standard frames for each cluster are defined. For the in cluster, the momenta in the standard frame are (standard-frame quantities are indexed by a zero):

$$p_1^{(0)} = (E, 0, 0, -q), \quad k_1^{(0)} = (\omega, 0, 0, q), \quad (2.1)$$

$$s = (p_1 + k_1)^2 = W^2, \quad (2.2)$$

$$q = \Delta^{1/2}(W^2, m^2, \lambda^2)/2W, \quad (2.3)$$

$$\Delta(x, y, z) = x^2 + y^2 + z^2 - 2xy - 2yz - 2zx. \quad (2.4)$$

The standard frame for the out cluster is defined analogously. The two frames are connected by an element of the little group of $P = p_1 + k_1 = (W, \vec{0})$ which is a rotation specified by the Euler angles $\gamma_2, \beta, \gamma_1$. The rotations γ_2, γ_1 are around the z axes of the out and in standard frames and do not change the momenta, and only introduce phase factors through the wave functions, and may be ignored. Hence, quite generally, we can choose the following frame to calculate the amplitude:

$$p_1 = (E, -q \sin\beta, 0, -q \cos\beta), \quad (2.5)$$

$$k_1 = (\omega, q \sin\beta, 0, q \cos\beta), \quad (2.6)$$

$$p_2 = (E, 0, 0, -q), \quad k_2 = (\omega, 0, 0, q). \quad (2.6)$$

The spinors and polarization vectors corresponding to the helicities τ, λ are, in the standard frame,

$$u_\tau(p_1^{(0)}) = \left(\frac{E+m}{2m}\right)^{1/2} \begin{pmatrix} \chi_{-\tau}^{(0)} \\ \frac{2\tau q}{E+m} \chi_{-\tau}^{(0)} \end{pmatrix}, \quad (2.7)$$

where

$$\begin{aligned} \chi_{+1/2}^{(0)} &= \begin{pmatrix} 1 \\ 0 \end{pmatrix}, & \chi_{-1/2}^{(0)} &= \begin{pmatrix} 0 \\ 1 \end{pmatrix}, \\ \epsilon_{\lambda_1}^{(0)}(k_1^{(0)}) &= (0, -1/\sqrt{2}, -i/\sqrt{2}, 0) & (\lambda_1 = +1) \\ &= (0, 0, 0, \lambda/\omega) & (\lambda_1 = 0) \\ &= (0, 1/\sqrt{2}, -i/\sqrt{2}, 0) & (\lambda_1 = -1), \end{aligned} \quad (2.8)$$

where we have used current conservation to eliminate the time component of $\epsilon(k)$. The following gauge simplifies calculations¹:

$$\epsilon_1 \cdot \Gamma_1 = \gamma \cdot \epsilon_1 - \gamma \cdot k_1 (\epsilon_1 \cdot A / k_1 \cdot A), \quad (2.9)$$

$$\epsilon_2^* \cdot \Gamma_2 = \gamma \cdot \epsilon_2^* - \gamma \cdot k_2 (\epsilon_2^* \cdot B / k_2 \cdot B), \quad (2.10)$$

where A is any vector which is not rotated through the angle β , (e.g., p_2, k_2) and B is any vector which is rotated through the angle β , (e.g., p_1, k_1). With this choice of gauge, as

$$z = \cos\beta \rightarrow \infty,$$

we find³

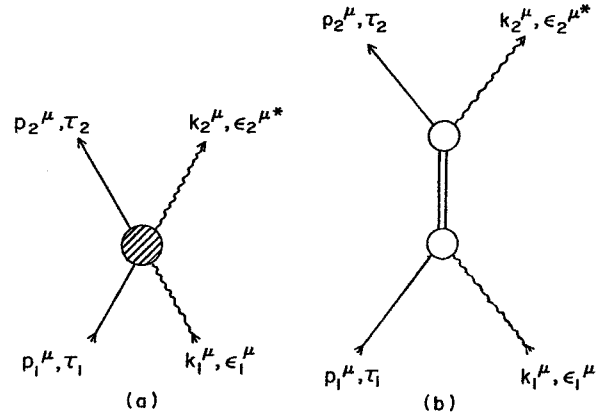


FIG. 1. (a) Momenta and polarizations of particles involved; (b) separation into "out" and "in" clusters.

$$\begin{aligned} \epsilon_1 \cdot \Gamma_{1z} &\sim \infty \text{ const}, \\ \epsilon_2^* \cdot \Gamma_{2z} &\sim \infty \text{ const}, \end{aligned} \quad (2.11)$$

and the contributions of "crossed" diagrams vanish compared to those of the "uncrossed" diagrams³ (Fig. 2).

Hence, the amplitude is, in lowest order, given by

$$T_{z \sim \infty} \sim g^2 \bar{u}(p_2) \epsilon_2^* \cdot \Gamma_2 (\gamma \cdot p_1 + \gamma \cdot k_1 - m)^{-1} \epsilon_1 \cdot \Gamma_1 u(p_1). \quad (2.12)$$

To obtain the amplitude for scattering through the positive-parity channel, we introduce the projection operator $\frac{1}{2}(1 + \Pi)$, where Π is the parity operator acting on the in state, which takes $u(p_1) \rightarrow \gamma^0 u(p_1)$ and $p_1 \rightarrow \bar{p}_1 = (E, -\vec{p}_1)$, etc:

$$\epsilon_2^* \cdot \Gamma_2 \frac{\Pi}{2} [\gamma \cdot \epsilon_2^* - \gamma \cdot k_2 (B \cdot \epsilon_2^* / B \cdot k_2)] \rightarrow \epsilon_2^* \cdot \Gamma_2, \quad (2.13)$$

$$\begin{aligned} \epsilon_1 \cdot \Gamma_1 u(p_1) \frac{\Pi}{2} [-\gamma \cdot \epsilon_1 + \gamma \cdot \bar{k}_1 (A \cdot \epsilon_1 / A \cdot \bar{k}_1)] &\rightarrow \gamma^0 u(p_1) \\ z \sim \infty &\gamma^0 \epsilon_1 \cdot \Gamma_1 u(p_1). \end{aligned} \quad (2.14)$$

Hence,

$$T_{z \sim \infty}^{(+)} \sim g^2 \bar{u}(p_2) \epsilon_2^* \cdot \Gamma_2 (W \gamma^0 - m)^{-1} \frac{1}{2} (1 + \gamma^0) \epsilon_1 \cdot \Gamma_1 u(p_1). \quad (2.15)$$

But

$$\begin{aligned} \frac{1}{2} (1 + \gamma^0) \epsilon_1 \cdot \Gamma_1 u(p_1) &= \frac{1}{2} (1 + \gamma^0) e^{-i(\beta/2)\alpha_y} \left(\gamma \cdot \epsilon_1^{(0)} - \gamma \cdot k_1^{(0)} \frac{\epsilon_1 \cdot A}{k_1 \cdot A} \right) u(p_1^{(0)}) \\ z \sim \infty &\frac{1}{2} (1 + \gamma^0) e^{-i(\beta/2)\alpha_y} \left(\gamma \cdot \epsilon_1^{(0)} - \gamma \cdot k_1^{(0)} \frac{\epsilon_1^{(0)} \cdot \alpha}{k_1^{(0)} \cdot \alpha} \right) u(p_1^{(0)}), \end{aligned} \quad (2.16)$$

where

$$\alpha = (0, -i, 0, 1). \quad (2.17)$$

This reduces to

$$\frac{1}{2}(1+\gamma^0)\epsilon_1 \cdot \Gamma_1 u(p_1) \underset{z \rightarrow \infty}{\sim} e^{-i(\beta/2)\sigma_y} \begin{pmatrix} \chi_{\lambda_1 \tau_1}(W) \\ 0 \end{pmatrix}, \quad (2.18)$$

where

$$\begin{aligned} \chi_{1\frac{1}{2}}(W) &= \frac{E-m-\omega}{[4m(E-m)]^{1/2}} \begin{pmatrix} 1 \\ 0 \end{pmatrix}, \\ \chi_{0\frac{1}{2}}(W) &= \frac{-\lambda}{[2m(E-m)]^{1/2}} \begin{pmatrix} 0 \\ 1 \end{pmatrix}, \\ \chi_{-1\frac{1}{2}}(W) &= \frac{W-m}{[4m(E-m)]^{1/2}} \begin{pmatrix} 1 \\ 0 \end{pmatrix}. \end{aligned} \quad (2.19)$$

Similarly,

$$\begin{aligned} \bar{u}(p_2)\epsilon_2^* \cdot \Gamma_2 \frac{1}{2}(1+\gamma^0) e^{-i(\beta/2)\sigma_y} \underset{z \rightarrow \infty}{\sim} \bar{u}(p_2^{(0)}) \left(\gamma \cdot \epsilon_2^{(0)*} - \gamma \cdot k_2^{(0)} \frac{\epsilon_2^{(0)*} \cdot \alpha^*}{k_2^{(0)} \cdot \alpha^*} \right) \frac{1}{2}(1+\gamma^0) e^{-i(\beta/2)\sigma_y}, \\ \underset{z \rightarrow \infty}{\sim} (\chi_{\lambda_2 \tau_2}^\dagger(W), 0) e^{-i(\beta/2)\sigma_y}. \end{aligned} \quad (2.20)$$

Hence, finally,

$$\begin{aligned} T_{\lambda_2 \tau_2, \lambda_1 \tau_1}^{(+)} \underset{z \rightarrow \infty}{\sim} g^2 \chi_{\lambda_2 \tau_2}^\dagger(W) (W-m)^{-1} e^{-i(\beta/2)\sigma_y} \chi_{\lambda_1 \tau_1}(W) \\ \underset{z \rightarrow \infty}{\sim} g^2 \beta_{\lambda_2 \tau_2}^*(W) \beta_{\lambda_1 \tau_1}(W) (W-m)^{-1} (\frac{1}{2}z)^{1/2}, \end{aligned} \quad (2.21)$$

where

$$\beta_{\lambda \tau}(W) = (1, -i)\chi_{\lambda \tau}(W). \quad (2.22)$$

The asymptotic behavior due to a single Regge pole $\alpha(s)$ is given by

$$\begin{aligned} T_{\lambda_3 \lambda_4, \lambda_1 \lambda_2}(s, t) \underset{z_s \rightarrow \infty}{\sim} \frac{-\pi \Gamma(1+2\alpha)}{\sin \pi(\alpha - \frac{1}{2})} \gamma_{34}(s) \gamma_{12}(s) d_{\lambda \mu}^{\alpha(s)}(z_s) \\ (\lambda = \lambda_1 - \lambda_2; \mu = \lambda_3 - \lambda_4). \end{aligned} \quad (2.23)$$

Using the property

$$\begin{aligned} d_{\lambda \mu}^{\alpha}(z) \underset{z \rightarrow \infty}{\sim} \frac{i^\lambda}{[\Gamma(\alpha + \lambda + 1)\Gamma(\alpha - \lambda + 1)]^{1/2}} \\ \times \frac{i^{-\mu} (\frac{1}{2}z)^\alpha}{[\Gamma(\alpha + \mu + 1)\Gamma(\alpha - \mu + 1)]^{1/2}}, \end{aligned} \quad (2.24)$$

and absorbing the factors in (2.24) into the functions γ_{34} and γ_{12} , we have

$$T_{34,12}(s, t) \underset{z \rightarrow \infty}{\sim} \frac{\tilde{\gamma}_{34}^*(s) \tilde{\gamma}_{12}(s)}{\sin \pi(\alpha - \frac{1}{2})} (\frac{1}{2}z)^{\alpha(s)}. \quad (2.25)$$

Using the lowest-order form for the trajectory

$$\alpha(W) = \frac{1}{2} + g^2(W-m)f(W) \cdots, \quad (2.26)$$

Eq.(2.25) gives, in lowest order, the following result:

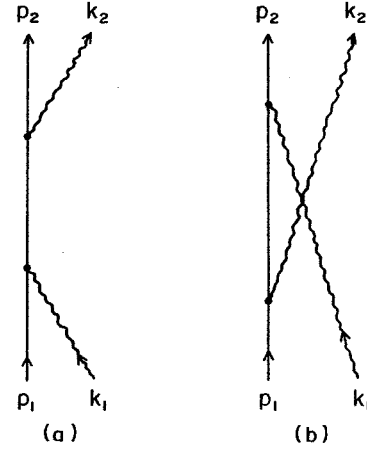


FIG. 2. (a) The uncrossed graph; (b) the crossed graph.

$$T_{34,12}(s, t) \underset{z \rightarrow \infty}{\sim} \beta_{34}^*(s) \beta_{12}(s) (W-m)^{-1} (\frac{1}{2}z)^{1/2}. \quad (2.27)$$

Comparing (2.27) and (2.21), we find that the Born approximation is consistent with Regge behavior, $\alpha(s) - \frac{1}{2}$ as $g^2 \rightarrow 0$, as found in (1). However, in (1) the factors $(\sqrt{2} \cos \frac{1}{2}\beta)^{-|\lambda+\mu|}$ and $(\sqrt{2} \sin \frac{1}{2}\beta)^{-|\lambda-\mu|}$ were extracted while defining definite-parity amplitudes. In our treatment, these factors have not been extracted, so that all the amplitudes (sense-sense, sense-nonsense, nonsense-nonsense) go as $z^{1/2}$.

III. THE AMPLITUDE $N\gamma \rightarrow N\gamma\gamma$ AND ITS SINGLE REGGE LIMIT

In this case, the standard frame for the in cluster (Fig. 3) $p_1 k_1$ is the same as in Sec. II. The standard frame for the out cluster is specified below:

$$p_2^{(0)} = (E_2, 0, 0, -p_{2z}^{(0)}), \quad (3.1)$$

$$l_2^{(0)} = (\omega_2, l_{2x}^{(0)}, 0, l_{2z}^{(0)}), \quad (3.2)$$

$$l_3^{(0)} = (\omega_3, -l_{3x}^{(0)}, 0, p_{2z}^{(0)} - l_{2z}^{(0)}), \quad (3.3)$$

and

$$E_2 + \omega_2 + \omega_3 = \sqrt{s} = W.$$

As in Sec. II, a rotation about the z axis of the state $|p_1^{(0)}, k_1^{(0)}\rangle$ only introduces a phase factor and may be disregarded. But the rotation about the z axis of (3.1)–(3.3) changes $l_2^{(0)}, l_3^{(0)}$, and is nontrivial. Hence, we calculate the amplitude in the frame

$$p_1 = (E, -q \sin \beta, 0, -q \cos \beta), \quad (3.4)$$

$$k_1 = (\omega, q \sin \beta, 0, q \cos \beta),$$

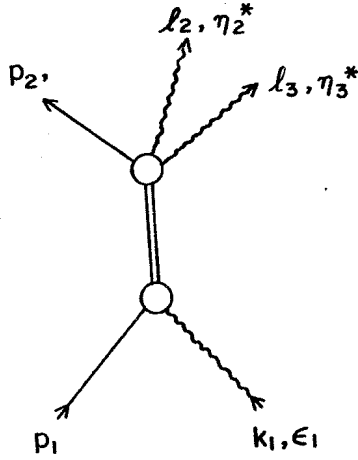


FIG. 3. "In" and "out" clusters.

$$\begin{aligned}
 p_2 &= (E_2, 0, 0, -p_{2z}^{(0)}), \\
 l_2 &= \Lambda_z(\gamma_2) \cdot l_2^{(0)}, \\
 l_3 &= \Lambda_z(\gamma_2) \cdot l_3^{(0)},
 \end{aligned}
 \tag{3.5}$$

where $\Lambda_z(\gamma_2)$ is the transformation matrix for z rotation through the angle γ_2 .

The gauge chosen is

$$\epsilon_1 \cdot \Gamma_1 = \gamma \cdot \epsilon_1 - \gamma \cdot k_1 (\epsilon_1 \cdot A / k_1 \cdot A),
 \tag{3.6}$$

$$\eta_2^* \cdot \Omega_2 = \gamma \cdot \eta_2^* - \gamma \cdot l_2 (\eta_2^* \cdot B / l_2 \cdot B),
 \tag{3.7}$$

$$G_3^{(0)} = \bar{u}(p_2^{(0)}) [\eta_2^{(0)*} \cdot \Omega_2^{(0)} (\gamma \cdot p_2^{(0)} + \gamma \cdot l_2^{(0)} - m)^{-1} \eta_3^{(0)} \cdot \Omega_3^{(0)} + \eta_3^{(0)*} \cdot \Omega_3^{(0)} (\gamma \cdot p_2^{(0)} + \gamma \cdot l_3^{(0)} - m)^{-1} \eta_2^{(0)*} \cdot \Omega_2^{(0)}] e^{i(\gamma_2/2)\sigma_z}
 \begin{pmatrix} 1 \\ i \\ 0 \\ 0 \end{pmatrix}
 \tag{3.10}$$

where

$$\eta_i^{(0)*} \cdot \Omega_i^{(0)} = \gamma \cdot \eta_i^{(0)*} - \gamma \cdot l_i^{(0)} (\eta_i^{(0)*} \cdot b / l_i^{(0)} \cdot b),
 \tag{3.11}$$

$$b = (0, i \cos \gamma_2, -i \sin \gamma_2, 1).
 \tag{3.12}$$

The form (3.9) exhibits $z^{1/2}$ behavior and the pole $(W - m)^{-1}$. Further, the factored residue $\beta_{\lambda_1 \tau_1}(W)$ is the same as found in Sec. II. The factor $G_3^{(0)}$ which depends only on the variables of the out cluster describes the Reggeon- $N\gamma\gamma$ coupling.

IV. SINGLE REGGE LIMIT $N\gamma\gamma \rightarrow N\gamma\gamma$

The standard frames for the in and out clusters (Fig. 5) are chosen as in Sec. III for the out cluster. In this case, both the z rotations γ_1, γ_2 are non-trivial and must be considered. Thus, the amplitude is calculated in the frame

$$|p_1 k_1 k_2\rangle = R_y(\beta) R_z(\gamma_1) |p_1^{(0)} k_1^{(0)} k_2^{(0)}\rangle,
 \tag{4.1}$$

$$|p_2 l_2 l_3\rangle = R_z(\gamma_2) |p_2^{(0)} l_2^{(0)} l_3^{(0)}\rangle,
 \tag{4.2}$$

$$p_1 + k_1 + k_2 = p_2 + l_2 + l_3 = (W, \vec{0}).$$

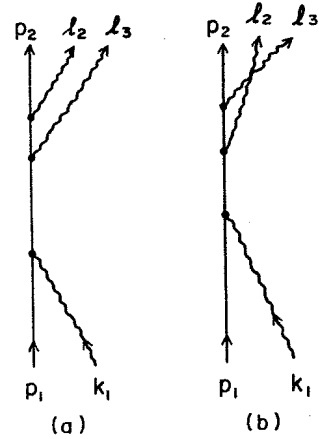


FIG. 4. The dominant, "uncrossed" graphs.

$$\eta_3^* \cdot \Omega_3 = \gamma \cdot \eta_3^* - \gamma \cdot l_3 (\eta_3^* \cdot B' / l_3 \cdot B'),
 \tag{3.8}$$

where A is an "unrotated" vector and B, B' are "rotated" vectors. In this gauge, the "uncrossed" graphs dominate⁴ (Fig. 4).

Introducing the positive-parity projection operator, taking the limit $z \rightarrow \infty$, and separating out the rotation operator which takes p_2, l_2, l_3 into the standard frame, we have

$$T^{(+)}_{z \rightarrow \infty} \sim g^3 G_3^{(0)} \cdot (\frac{1}{2}z)^{1/2} (W - m)^{-1} \beta_{\lambda_1 \tau_1}(W),
 \tag{3.9}$$

where $\beta_{\lambda_1 \tau_1}(W)$ is the same as in (2.22), and

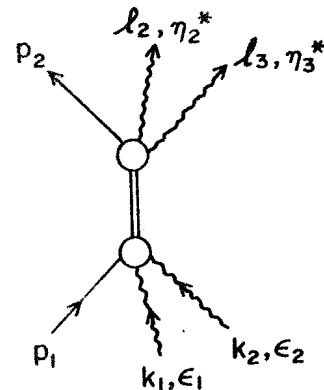


FIG. 5. Clusters for $N\gamma\gamma \rightarrow N\gamma\gamma$.

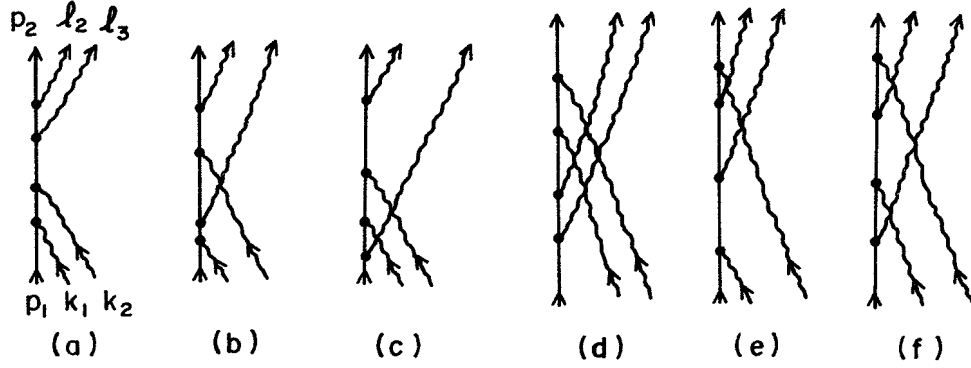


FIG. 6. The six classes of diagrams for $N\gamma\gamma \rightarrow N\gamma\gamma$. The four members in each class are obtained by the independent interchanges $l_2 \leftrightarrow l_3$; $k_1 \leftrightarrow k_2$. Class-(a) graphs are "uncrossed" and dominate in the limit $z \rightarrow \infty$.

The gauge is again chosen so as to eliminate the crossed diagrams⁴ as $z = \cos\beta \rightarrow \infty$:

$$\epsilon_i \cdot \Gamma_i = \gamma \cdot \epsilon_i - \gamma \cdot k_i (A_i \cdot \epsilon_i / A_i \cdot k_i), \quad (4.3)$$

where A_i is an "unrotated" vector (e.g., p_2, l_2, l_3) and

$$\eta_i^* \cdot \Omega_i = \gamma \cdot \eta_i^* - \gamma \cdot l_i (B_i \cdot \eta_i^* / B_i \cdot l_i), \quad (4.4)$$

where B_i is a "rotated" vector (e.g., p_1, k_1, k_2).

The 24 possible lowest-order diagrams fall naturally into six classes of four diagrams each (Fig. 6), only one class of which survives [Fig. 6(a)] in the limit $z \rightarrow \infty$ (uncrossed type).⁴ Hence,

$$T_{z \rightarrow \infty} \sim g^4 F_A \cdot (W\gamma^0 - m)^{-1} \cdot F_B, \quad (4.5)$$

where

$$F_A = \bar{u}(p_2) [\eta_2^* \cdot \Omega_2 (\gamma \cdot p_2 + \gamma \cdot l_2 - m)^{-1} \eta_3^* \cdot \Omega_3 + \eta_3^* \cdot \Omega_3 (\gamma \cdot p_2 + \gamma \cdot l_3 - m)^{-1} \eta_2^* \cdot \Omega_2] \quad (4.6)$$

and

$$F_B = [\epsilon_2 \cdot \Gamma_2 (\gamma \cdot p_1 + \gamma \cdot k_1 - m)^{-1} \epsilon_1 \cdot \Gamma_1 + \epsilon_1 \cdot \Gamma_1 (\gamma \cdot p_1 + \gamma \cdot k_2 - m)^{-1} \epsilon_2 \cdot \Gamma_2] u(p_1). \quad (4.7)$$

The positive-parity projection operator can be introduced as before, and taking the limit $z \rightarrow \infty$, separating out the rotations γ_1, γ_2 , we have

$$T_{z \rightarrow \infty}^{(+)} \sim g^4 G_A^{(0)} (W - m)^{-1} (\frac{1}{2}z)^{1/2} G_B^{(0)}, \quad (4.8)$$

where

$$G_A^{(0)} = \bar{u}(p_2) [\eta_2^{(0)*} \cdot \Omega_2^{(0)} (\gamma \cdot p_2^{(0)} + \gamma \cdot l_2^{(0)} - m)^{-1} \eta_3^{(0)*} \cdot \Omega_3^{(0)} + \eta_3^{(0)*} \cdot \Omega_3^{(0)} (\gamma \cdot p_2^{(0)} + \gamma \cdot l_3^{(0)} - m)^{-1} \eta_2^{(0)*} \cdot \Omega_2^{(0)}] e^{(i/2)\gamma_2 \sigma_z} \begin{bmatrix} 1 \\ i \\ 0 \\ 0 \end{bmatrix}, \quad (4.9)$$

where $\eta_i^{(0)*} \cdot \Omega_i^{(0)}$ are defined in (3.11), and

$$G_B^{(0)} = (1, -i, 0, 0) e^{-i(\gamma_1/2)\sigma_z} [\epsilon_2^{(0)} \cdot \Gamma_2^{(0)} (\gamma \cdot p_1^{(0)} + \gamma \cdot k_1^{(0)} - m)^{-1} \epsilon_1^{(0)} \cdot \Gamma_1^{(0)} + \epsilon_1^{(0)} \cdot \Gamma_1^{(0)} (\gamma \cdot p_1^{(0)} + \gamma \cdot k_2^{(0)} - m)^{-1} \epsilon_2^{(0)} \cdot \Gamma_2^{(0)}] u(p_1^{(0)}), \quad (4.10)$$

where

$$\epsilon_i^{(0)} \cdot \Gamma_i^{(0)} = \gamma \cdot \epsilon_i^{(0)} - \gamma \cdot k_i^{(0)} (\epsilon_i^{(0)} \cdot c / k_i^{(0)} \cdot c), \quad (4.11)$$

$$c = (0, -i \cos\gamma_1, i \sin\gamma_1, 1). \quad (4.12)$$

The form (4.8) shows $z^{1/2}$ behavior, the pole $(W - m)^{-1}$, and two factors $G_A^{(0)}, G_B^{(0)}$, which depend only on their cluster variables, and are identical in form (except for complex conjugation) with (3.12). This shows that the logical circle of factorization closes, and that the coupling Reggeon $\rightarrow N\gamma\gamma$ can be consistently and uniquely identified.

V. DOUBLE REGGE LIMIT FOR $N\gamma \rightarrow N\gamma\gamma$

The form of the amplitude obtained in Sec. III can be further investigated for Regge behavior and factorization, by subdividing the out cluster (Fig. 7). The frame is specified in more detail for this purpose.

In frame 1 (used in Sec. III)

$$\begin{aligned} p_1 + k_1 &= (W, \vec{0}), \\ |p_1 k_1\rangle &= R_y(\beta) |p_1^{(0)} k_1^{(0)}\rangle. \end{aligned} \quad (5.1)$$

A boost along the z axis of magnitude ξ takes frame 1 to frame 2 (where quantities are primed), the center-of-mass frame of the p_2, l_2 cluster:

$$p'_1 + k'_1 = P' = (W \cosh \xi, 0, 0, W \sinh \xi), \quad (5.2)$$

$$l'_3 = [(\lambda^2 + W^2 \sinh^2 \xi)^{1/2} = \omega'_3, 0, 0, W \sinh \xi = q'_3], \quad (5.3)$$

$$p'_2 + l'_2 = (W \cosh \xi - \omega'_3 = W', \vec{0}), \quad (5.4)$$

$$\begin{aligned} l'_2 &= (\omega'_2, q' \sin \beta' \cos \gamma', q' \sin \beta' \sin \gamma', q' \cos \beta') \\ &= \Lambda_z(\gamma') \cdot \Lambda_y(\beta') \cdot l_2^{(0)}, \end{aligned} \quad (5.5)$$

$$p'_2 = (E'_2, -\vec{l}'_2), \quad (5.6)$$

and

$$q' = \Delta^{1/2}(W'^2, m^2, \lambda^2)/2W'. \quad (5.7)$$

The five independent variables are

$$W, \beta, W', \beta', \gamma',$$

with

$$\cosh \xi = (W^2 + W'^2 - \lambda^2)/2WW'. \quad (5.8)$$

γ' can be shown to be the usual Toller angle.⁵

In the limit $z = \cos \beta \rightarrow \infty$, the result of Sec. III was

$$T^{(+)}_{z \rightarrow \infty} \sim g^3 G_3(\frac{1}{2}z)^{1/2} (W - m)^{-1} \beta_{\lambda_1 \tau_1}(W), \quad (5.9)$$

where

$$G_3 = \bar{u}(p_2) [\eta_2^* \cdot \Omega_2(\gamma \cdot p_2 + \gamma \cdot l_2 - m)^{-1} \eta_3^* \cdot \Omega_3 + \eta_3^* \cdot \Omega_3(\gamma \cdot p_2 + \gamma \cdot l_3 - m)^{-1} \eta_2^* \cdot \Omega_2] \begin{pmatrix} 1 \\ i \\ 0 \\ 0 \end{pmatrix} \quad (5.10)$$

[note that the rotation γ_2 has not been extracted in (5.10)].

Using the properties of the boost operator

$$S_3(\xi) = e^{\alpha_3 \xi / 2} = \begin{pmatrix} \cosh \frac{1}{2} \xi & \sigma_z \sinh \frac{1}{2} \xi \\ \sigma_z \sinh \frac{1}{2} \xi & \cosh \frac{1}{2} \xi \end{pmatrix}, \quad (5.11)$$

we have

$$T^{(+)}_{z \rightarrow \infty} \sim g^3 \bar{u}(p'_2) [\eta_2^{*'} \cdot \Omega_2(\gamma \cdot p'_2 + \gamma \cdot l'_2 - m)^{-1} \eta_3^{*'} \cdot \Omega_3 + \eta_3^{*'} \cdot \Omega_3(\gamma \cdot p'_2 + \gamma \cdot l'_3 - m)^{-1} \eta_2^{*'} \cdot \Omega_2] e^{\alpha_3 \xi / 2} \begin{pmatrix} 1 \\ i \\ 0 \\ 0 \end{pmatrix}, \quad (5.12)$$

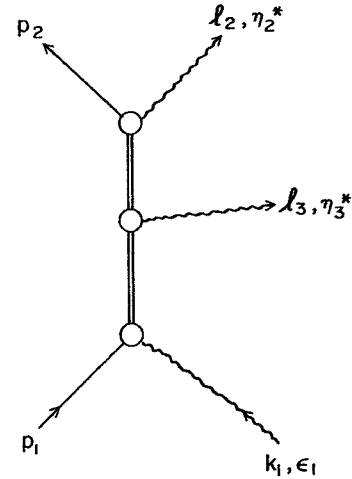


FIG. 7. Clusters for the double Regge limit of $N\gamma \rightarrow N\gamma\gamma$.

where

$$\eta_i^{*'} \cdot \Omega_i' = \gamma \cdot \eta_i^{*'} - \gamma \cdot l_i' (\eta_i^{*'} \cdot b' / l_i' \cdot b'), \quad (5.13)$$

$$b' = (\sinh \xi, i, 0, \cosh \xi). \quad (5.14)$$

We now introduce the positive-parity projection operator on the state $|p_2' l_2'\rangle$ in its c.m. frame (frame 2) and take the limit $z' = \cos \beta' \rightarrow \infty$. After some manipulations, we find

$$T^{(+,+)}_{z, z' \rightarrow \infty} g^{-3} \beta_{\lambda_2'}^{*'} (W') (\frac{1}{2} z')^{1/2} (W' - m)^{-1} \Gamma_{\lambda_3'} (\frac{1}{2} z')^{1/2} (W - m)^{-1} \beta_{\lambda_1'} (W), \quad (5.15)$$

where β_{λ_T} is defined in (2.22), and the quantity Γ_{λ_3} is given by

$$\Gamma_{+1} = e^{-i\gamma'/2} \left[i\sqrt{2} \sinh \frac{1}{2} \xi + \frac{\sin \frac{1}{2} \gamma'}{\sqrt{2} \sinh \frac{1}{2} \xi} \left(\frac{W' - m}{W} e^{-i\gamma'/2} - \frac{W - m}{W'} e^{i\gamma'/2} \right) \right], \quad (5.16)$$

$$\Gamma_0 = - \frac{i\lambda \sin \frac{1}{2} \gamma' (W + W' - m)}{W W' \sinh \frac{1}{2} \xi}, \quad (5.17)$$

$$\Gamma_{-1} = e^{i\gamma'/2} \left[i\sqrt{2} \sinh \frac{1}{2} \xi - \frac{\sin \frac{1}{2} \gamma'}{\sqrt{2} \sinh \frac{1}{2} \xi} \left(\frac{W' - m}{W} e^{i\gamma'/2} - \frac{W - m}{W'} e^{-i\gamma'/2} \right) \right]. \quad (5.18)$$

$\Gamma_\lambda(W, W', \gamma')$ may be regarded as the Reggeon-Reggeon-photon coupling and is symmetrical with respect to the variables of the two Reggeons. The dependence of this coupling on the Toller angle has been studied by Tan and Wang,⁶ who conjecture that $\sum_\lambda |\Gamma_\lambda|^2$ should be independent of γ' when either W or $W' \rightarrow 0$. Our coupling does not satisfy this conjecture, possibly because of the extra complications in fermion kinematics.

VI. CONCLUSION

Reggeization of the nucleon in this model was originally established¹ for the two-body process $N\gamma \rightarrow N\gamma$. The multibody processes $N\gamma \rightarrow N\gamma\gamma$ and $N\gamma\gamma \rightarrow N\gamma\gamma$ have been shown to have the same Regge pole in the tree-diagram approximation. The residues factorize and the couplings $N\gamma$ -Reggeon, $N\gamma\gamma$ -Reggeon can be identified. The double Regge limit of $N\gamma \rightarrow N\gamma\gamma$ also shows the same pole; and an additional coupling Reggeon- γ -Reggeon can be identified. The method can be generalized to processes with arbitrary number of photons in the initial and final states. Thus, in the tree-diagram approximation, at least, the generalized Reggeization of S -matrix elements has been found to be true. However, higher-order calculations of these multibody S -matrix elements are necessary to bring the proof to the level established for the two-body process in Ref. 1.

ACKNOWLEDGMENT

I am grateful to Professor D.Z. Freedman for suggesting this problem and for valuable discussions.

APPENDIX A

Let the vector $a^{(0)}$ be rotated through an angle β about the y axis. Then, as $\cos \beta = z \rightarrow \infty$,

$$\vec{a}_{z \rightarrow \infty} \sim z(a_1^{(0)} + ia_3^{(0)})(\hat{x} - iz\hat{z}). \quad (A1)$$

Hence, in general,

$$a_{z \rightarrow \infty} \sim z\alpha(a^{(0)} \cdot \rho), \quad (A2)$$

where

$$\rho = (0, -i, 0, 1), \quad \alpha = (0, i, 0, 1). \quad (A3)$$

Hence,

$$\begin{aligned} \epsilon_1 \cdot \Gamma_{1z \rightarrow \infty} \gamma \cdot \epsilon_1 - \gamma \cdot k_1 (\epsilon_1^{(0)} \cdot \rho / k_1^{(0)} \cdot \rho) \\ z \rightarrow \infty \left(\begin{array}{cc} -\omega_1 (\epsilon_1^{(0)} \cdot \rho / k_1^{(0)} \cdot \rho) & -\vec{\sigma} \cdot [\vec{\epsilon}_1 - \vec{k}_1 (\epsilon_1^{(0)} \cdot \rho / k_1^{(0)} \cdot \rho)] \\ + \dots & + \dots \end{array} \right) \end{aligned} \quad (A4)$$

But

$$\omega_1(\epsilon_1^{(0)} \cdot \rho / k_1^{(0)} \cdot \rho)_{z \rightarrow \infty} \text{const} \quad (\text{A5})$$

and

$$\bar{\sigma} \cdot [\bar{\epsilon}_1 - \bar{k}_1(\epsilon_1^{(0)} \rho / k_1^{(0)} \cdot \rho)]_{z \rightarrow \infty} - z[\epsilon_1^{(0)} \cdot \rho \bar{\sigma} \cdot \bar{\alpha} - k_1^{(0)} \cdot \rho \bar{\sigma} \cdot \bar{\alpha}(\epsilon_1^{(0)} \cdot \rho / k_1^{(0)} \cdot \rho)]_{z \rightarrow \infty} \text{const.} \quad (\text{A6})$$

Hence,

$$\epsilon_1 \cdot \Gamma_1, \epsilon_2^* \cdot \Gamma_2_{z \rightarrow \infty} \text{const.} \quad (\text{A7})$$

The contribution of the crossed graph [Fig. 2(b)] is

$$\begin{aligned} T_b &\sim \bar{u}(p_2) \epsilon_1 \cdot \Gamma_1 (\gamma \cdot p_1 - \gamma \cdot k_2 - m)^{-1} \epsilon_2^* \cdot \Gamma_2 u(p_1) \\ &\stackrel{z \rightarrow \infty}{\sim} (-\frac{1}{2} p_1 \cdot k_2) \bar{u}(p_2) \epsilon_1 \cdot \Gamma_1 (\gamma \cdot p_1 + \gamma \cdot k_2 + m) \epsilon_2^* \cdot \Gamma_2 u(p_1) \\ &\stackrel{z \rightarrow \infty}{\sim} \bar{u}(p_2) \epsilon_1 \cdot \Gamma_1 [B \cdot \epsilon_2^* / B \cdot k_2 - (p_1 \cdot \epsilon_2^* / p_1 \cdot k_2) + O(z^{-1})] u(p_1) \\ &\stackrel{z \rightarrow \infty}{\sim} O(1) O(1) O(z^{-1}) O(z^{1/2}) \\ &\stackrel{z \rightarrow \infty}{\sim} O(z^{-1/2}), \end{aligned} \quad (\text{A8})$$

since

$$B_{z \rightarrow \infty} - z \alpha(\rho \cdot B^{(0)}) \quad (\text{A9})$$

and we have used the property

$$(\gamma \cdot p_1 - m) u(p_1) = 0. \quad (\text{A10})$$

APPENDIX B

The diagrams are shown in Fig. 6. The gauge chosen is

$$\epsilon_i \cdot \Gamma_i = \gamma \cdot \epsilon_i - \gamma \cdot k_i (\epsilon_i \cdot A_i / k_i \cdot A), \quad i=1, 2 \quad (\text{B1})$$

(A_i is an "unrotated" vector)

$$\eta_i^* \cdot \Omega_i = \gamma \cdot \eta_i^* - \gamma \cdot l_i (\eta_i^* \cdot B_i / l_i \cdot B_i), \quad i=2, 3 \quad (\text{B2})$$

(B_i is a "rotated" vector).

The cluster p, k_1, k_2 is regarded as "rotated" with respect to the cluster p_2, l_2, l_3 by an angle β . In Appendix A it was shown that as $z = \cos \beta \rightarrow \infty$, $\epsilon_i \cdot \Gamma_i$ and $\eta_i^* \cdot \Omega_i \rightarrow \text{const.}$

The contribution of a graph of type (a) is typically

$$\begin{aligned} T_a &\sim \bar{u}(p_2) \eta_2^* \cdot \Omega_2 (\gamma \cdot p_2 + \gamma \cdot l_2 - m)^{-1} \eta_3^* \cdot \Omega_3 (\gamma \cdot p_1 + \gamma \cdot k_1 + \gamma \cdot k_2 - m)^{-1} \epsilon_2 \cdot \Gamma_2 (\gamma \cdot p_1 + \gamma \cdot k_1 - m)^{-1} \epsilon_1 \cdot \Gamma_1 u(p_1) \\ &\stackrel{z \rightarrow \infty}{\sim} O(1) O(1) O(1) O(1) O(1) O(1) O(1) O(1) O(z^{1/2}) \\ &\stackrel{z \rightarrow \infty}{\sim} O(z^{1/2}), \end{aligned} \quad (\text{B3})$$

since

$$R_y(\beta) = e^{-i(\beta/2)\sigma_y} \sim z^{1/2}.$$

The contribution of a graph of type (b) is

$$\begin{aligned} T_b &\sim \bar{u}(p_2) \eta_2^* \cdot \Omega_2 (\gamma \cdot p_2 + \gamma \cdot l_2 - m)^{-1} \epsilon_2 \cdot \Gamma_2 (\gamma \cdot p_2 + \gamma \cdot l_2 - \gamma \cdot k_2 - m)^{-1} \eta_3^* \cdot \Omega_3 (\gamma \cdot p_1 + \gamma \cdot k_1 - m)^{-1} \epsilon_1 \cdot \Gamma_1 u(p_1) \\ &\stackrel{z \rightarrow \infty}{\sim} O(1) O(1) O(1) O(1) \{ [(\eta_3^* \cdot p_1 / l_3 \cdot p_1) - (\eta_3^* \cdot (p_1 + k_1) / l_3 \cdot (p_1 + k_1)) + O(z^{-1})] (\gamma \cdot p_1 + \gamma \cdot k_1 - m)^{-1} \\ &\quad + O(z^{-1}) \cdot \eta_3^* \cdot \Omega_3 (\gamma \cdot p_1 + \gamma \cdot k_1 - \gamma \cdot l_3 - m) (\gamma \cdot p_1 + \gamma \cdot k_1 - m)^{-1} \} e^{-i(\beta/2)\sigma_y} (\epsilon_1 \cdot \Gamma_1)^0 u(p_1^{(0)}) \\ &\stackrel{z \rightarrow \infty}{\sim} O(z^{-1/2}). \end{aligned}$$

Similarly the graphs of class (c), (d), (e), and (f) may all be shown to go as $z^{-1/2}$, at least compared to $z^{1/2}$ for class-(a) graphs.

APPENDIX C

We refer to Fig. 7. The Toller angle ω_t , is defined by

$$\begin{aligned} \cos \omega_t &= - \left[\frac{(\vec{l}_2 \times \vec{p}_2) \cdot (\vec{k}_1 \times \vec{p}_1)}{|\vec{l}_2 \times \vec{p}_2| |\vec{k}_1 \times \vec{p}_1|} \right]_{\text{rest frame of } l_3} \\ &= + \left[\frac{P \cdot Q}{\sqrt{-P^2} \sqrt{-Q^2}} \right]_{\text{arbitrary frame}}, \end{aligned} \quad (\text{C1})$$

where

$$\begin{aligned} P^\mu &= \epsilon^{\mu\nu\lambda\sigma} l_{2\nu} p_{2\lambda} l_{3\sigma}, \\ Q^\mu &= \epsilon^{\mu\nu\lambda\sigma} k_{1\nu} p_{1\lambda} l_{3\sigma}. \end{aligned} \quad (\text{C2})$$

In the frame 2, the vectors $k'_1, p'_1, l'_3, l'_2, p'_2$ are

$$\begin{aligned} k'_1 &= (\omega \cosh \xi + q \cos \beta \sinh \xi, q \sin \beta, 0, q \cos \beta \cosh \xi + \omega \sinh \xi), \\ p'_1 &= (E \cosh \xi - q \cos \beta \sinh \xi, -q \sin \beta, 0, -q \cos \beta \cosh \xi + E \sinh \xi), \\ l'_3 &= (\omega'_3, 0, 0, W \sinh \xi), \\ p'_2 &= (E'_2, -q' \sin \beta' \cos \gamma', -q' \sin \beta' \sin \gamma', -q' \cos \beta'), \\ l'_2 &= (\omega'_2, q' \sin \beta' \cos \gamma', q' \sin \beta' \sin \gamma', q' \cos \beta'). \end{aligned} \quad (\text{C3})$$

Then the vectors P and Q are easily found to be

$$\begin{aligned} P &= (0, q' W W' \sinh \xi \sin \beta' \sin \gamma', -q W W' \sinh \xi \sin \beta' \cos \gamma', 0), \\ Q &= (0, 0, -q W W' \sinh \xi \sin \beta, 0), \end{aligned} \quad (\text{C4})$$

which gives

$$\cos \omega_t = \cos \gamma' \quad \text{or} \quad \omega_t = \gamma'. \quad (\text{C5})$$

Hence, γ' is the Toller angle.

*Work supported in part through funds provided by the Atomic Energy Commission under Contract No. AT(30-1)-2098.

¹(a) M. Gell-Mann, M. L. Goldberger, F. E. Low, E. Marx, and F. Zachariasen, Phys. Rev. **133**, B145 (1964); (b) M. Gell-Mann, M. L. Goldberger, F. E. Low, V. Singh, and F. Zachariasen, Phys. Rev. **133**, B161 (1964).

²J. B. Hartle and C. E. Jones, Phys. Rev. **184**, 1564 (1969), and references therein.

³Appendix A.

⁴Appendix B.

⁵Appendix C.

⁶C.-I. Tan and J. M. Wang, Phys. Rev. **185**, 1899 (1968).